

The sum

$$P_m^n \cos [(2\pi/L)(n_x + m_y)] + Q_m^n \sin [(2\pi/L)(n_x + m_y)] \tag{8}$$

Represents a single partial wave having a particular direction and wave length for which

$$(P_m^n)^2 + (Q_m^n)^2 = (C_m^n)^2 \tag{9}$$

C_m^n Is the amplitude of the partial wave, while the frequency of this wave is given as,

$$f_m^n = (n^2 + m^2)^{1/2} \tag{10}$$

The Fourier transform of magnetic data digitized in a square grid forms a square matrix which can be reduced to a set of average amplitudes depending only on the frequency [7]. These average amplitudes fully represent a spectrum from which the magnetic sources can be estimated.

In order to carry out Spectral analysis, the residual data of the study area were divided into forty nine (49) blocks containing 16 x16 data points. In doing this, it was ensured that essential parts of each anomaly were not cut by the blocks. The analysis was carried out using a Fourier based program Four pot developed and used by [10]. The software has taken care of some practical problems such as aliasing, Gibbs phenomenon and those associated with the odd and even symmetries of the real and imaginary parts of Fourier transformation, which arises when applying Discrete Fourier Transformation (DFT). The average depth to magnetic sources of each of the forty nine (49) blocks, which made up the study area were computed using the FORTRAN 99 program in the software. Table I summarizes the average depth computed from the blocks.

Table 1: Average Depth to Magnetic Sources in the study area (km)

Block 1 D1 = 0.732 D2 = 0.219	Block 2 D1 = 0.796 D2 = 0.217	Block 3 D1 = 0.949 D2 = 0.202	Block 4 D1 = 0.847 D2 = 0.157	Block 5 D1 = 0.437 D2 = 0.123	Block 6 D1 = 0.544	Block 7 D1 = 0.317
Block 8 D1 = 2.240 D2 = 0.378	Block 9 D1 = 2.141 D2 = 0.346	Block 10 D1 = 1.218 D2 = 0.202	Block 11 D1 = 0.722 D2 = 0.215	Block 12 D1 = 0.533	Block 13 D1 = 0.487	Block 14 D1 = 0.363
Block 15 D1 = 2.617 D2 = 0.261	Block 16 D1 = 1.435 D2 = 0.362	Block 17 D1 = 0.958 D2 = 0.257	Block 18 D1 = 0.524	Block 19 D1 = 0.451	Block 20 D1 = 0.412	Block 21 D1 = 0.227
Block 22 D1 = 1.578 D2 = 0.389	Block 23 D1 = 1.129 D2 = 0.440	Block 24 D1 = 0.934	Block 25 D1 = 0.583	Block 26 D1 = 0.488	Block 27 D1 = 0.375	Block 28 D1 = 0.301
Block 29 D1 = 0.183	Block 30 D1 = 0.485	Block 31 D1 = 0.422	Block 32 D1 = 0.280	Block 33 D1 = 0.488	Block 34 D1 = 0.430	Block 35 D1 = 0.604
Block 36 D1 = 0.570	Block 37 D1 = 0.330	Block 38 D1 = 0.363	Block 39 D1 = 0.320	Block 40 D1 = 0.773	Block 41 D1 = 0.523	Block 42 D1 = 0.830
Block 43 D1 = 0.778	Block 44 D1 = 0.579	Block 45 D1 = 0.691	Block 46 D1 = 0.442	Block 47 D1 = 0.630	Block 48 D1 = 0.445	Block 49 D1 = 0.970

4. Curie point Depth Estimation

The methods for estimating the depth extent of magnetic sources are classified into two categories; those that examine the shape of isolated anomalies [2] and those that examine the patterns of the anomalies [23]. However, both methods provide the relationship between the spectrum of

the magnetic anomalies and the depth to magnetic sources by transforming the spatial data into frequency domain. In this research, the method adopted is the later. To obtain the depth to Curie point, Spectral analysis of 2-dimensional Fourier transform of the aeromagnetic data has to be performed.

To carry out Spectral analysis, the study area was divided into sixteen overlapping blocks. Each block covers a square area of 64 by 64km, which represent a square grid of 32 by 32 data points except for the red numbered blocks which were padded and cosine tapered before Spectral evaluation for Curie and Heat flow assessments. In doing this, it was ensured that no essential part of the anomaly was cut-off by the blocks and each block was continued upward to eliminate shallow source (short wavelength and enhance the deep seated magnetic sources). The analysis was carried out using computer software FOURPOT version 1.0a, [10]. The software is a program designed for analysis of potential field data and based on its operations, The first step, is to estimate the depth to Centroid (Z_o) of the magnetic source from the slope of the longest wavelength part of the spectrum,

$$\ln \left[\frac{p(s)^{1/2}}{|s|} \right] = \ln A - 2\pi /s/Z_o \dots \dots \tag{11}$$

Where P(s) is the radially averaged power spectrum of the anomaly, /s/ is the wave number, and A is a constant. The second step is the estimation of the depth to the top boundary (Z_t) of that distribution from the slope of the second longest wavelength spectral segment [12].

$$\ln [P(s)^{1/2}] = \ln B - 2\pi /s/Z_t \dots \dots \tag{12}$$

Where B, is the sum of constants independent of /s/.

Then the basal depth (Z_b) of the magnetic source was calculated from the equation below,

$$Z_b = 2Z_o - Z_t \dots \dots \tag{13}$$

The obtained basal depth (Z_b) of magnetic sources in the study area is assumed to be the Curie point depth [2] and [12].

Table 2: Calculated Average Curie point depth from spectral analysis (km)

Block1 Z _O =12.520 Z _t =1.030 Z _b =24	Block2 Z _O =13.660 Z _t =1.220 Z _b =26	Block3 Z _O =14.980 Z _t =1.880 Z _b =28	Block4 Z _O =16.210 Z _t =4.980 Z _b =27
Block5 Z _O =14.230 Z _t =3.440 Z _b =25	Block6 Z _O =14.450 Z _t =2.890 Z _b =26	Block7 Z _O = 15.300 Z _t =3.220 Z _b =27	Block8 Z _O =13.891 Z _t =1.680 Z _b =26
Block9 Z _O =14.520 Z _t =2.200 Z _b =27	Block10 Z _O =15.100 Z _t =2.820 Z _b =27	Block11 Z _O =14.820 Z _t =1.430 Z _b =28	Block12 Z _O =16.100 Z _t =3.980 Z _b =28
Block13 Z _O = 15.200 Z _t =3.581 Z _b =27	Block14 Z _O =15.820 Z _t =3.440 Z _b =28	Block15 Z _O =14.000 Z _t =2.130 Z _b =26	Block16 Z _O =15.020 Z _t =3.080 Z _b =27

4.1. Estimation of Heat Flow and Geothermal Gradient

The heat flow and thermal gradient value was calculated in the study area, the calculation was expressed by Fourier's law with the following formula.

$$q = \lambda \frac{dT}{dZ} \tag{14}$$

Where *q* is the heat flow and λ is the coefficient of thermal conductivity. In this equation, it is assumed that the direction of the temperature variation is vertical and the temperature gradient dT/dZ is constant. According to “ref. [26]”, the Curie temperature (θ) was obtained from the Curie point depth (Z_b) and the thermal gradient dT/dZ using the following equation;

$$\theta = \left[\frac{dT}{dZ} \right] Z_b \tag{15}$$

Provided that there are no heat sources or heat sinks between the earth’s surface and the Curie – point depth, the surface temperature is 0°C and dT/dZ is constant. The Curie temperature depends on magnetic mineralogy. Although the Curie temperature of magnetite (Fe₂O₄), is approximately 580°C, in view of that, an increase in titanium (Ti) content of titanomagnetite (Fe_{2-x}Ti_xO₃) causes a reduction in Curie temperature [15]

In addition to that, from Equation (4) and Equation (5) a relationship was determined between the Curie point depth (Z_b) and the heat flow (*q*) as follows.

$$q = \lambda \left[\frac{\theta}{Z_b} \right] \tag{16}$$

In this equation, the Curie point depth is inversely proportional to the heat flow, [26]; [24] . In this research, the Curie point temperature of 580 °C and thermal conductivity of 2.5Wm⁻¹°C⁻¹ was used [15] in the study area. In order to compute the thermal gradient and heat flow of the region, Equation (6) was utilised. See Table 3 below.

Table 3: Calculated Heat flow and geothermal gradient from Curie depths.

Blocks	Z _O (km)	Z _t (km)	Z _b (km)	Geothermal(°C/km ⁻¹)	Heat flow(mW/m ⁻²)
1	12.520	1.030	24	24	61
2	13.660	1.220	26	22	56
3	14.980	1.880	28	21	53
4	16.210	4.980	27	21	53
5	14.230	3.440	25	23	58
6	14.450	2.890	26	22	56
7	15.300	3.220	27	21	53
8	13.891	1.680	26	22	56
9	14.520	2.200	27	22	55
10	15.100	2.820	27	21	53
11	14.820	1.430	28	21	53
12	16.100	3.980	28	21	53
13	15.200	3.581	27	22	55
14	15.820	3.440	28	21	53
15	14.000	2.130	26	23	58
16	15.020	3.080	27	21	55

4.3. Relationship between Curie Depth and Heat Flow

To investigate any possible relation between heat flow and the obtained Curie depths, we present the current results in Figure 7. Considering Curie depths and heat flow in the study area, Figure 6 shows that, the heat flow decreases with increasing Curie depth.

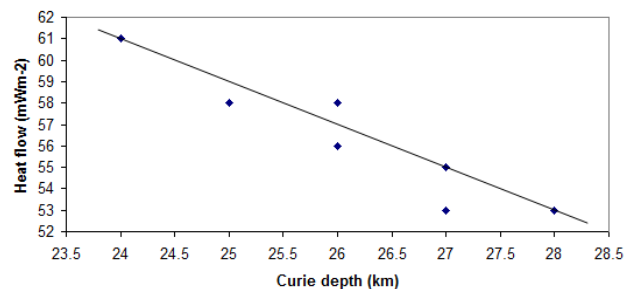


Figure 6: Heat flow versus Curie point depth in the study area.

However, Spectral analysis of aeromagnetic data in conjunction with these heat flow information revealed an almost inverse linear relation between heat flow and Curie depths. The curie depth obtained for the study area (Table 1) was used to construct the Curie isotherms which were delineated and are presented on Figure 7 below, this gives the direct nature of heat distribution in subsurface of the study area.

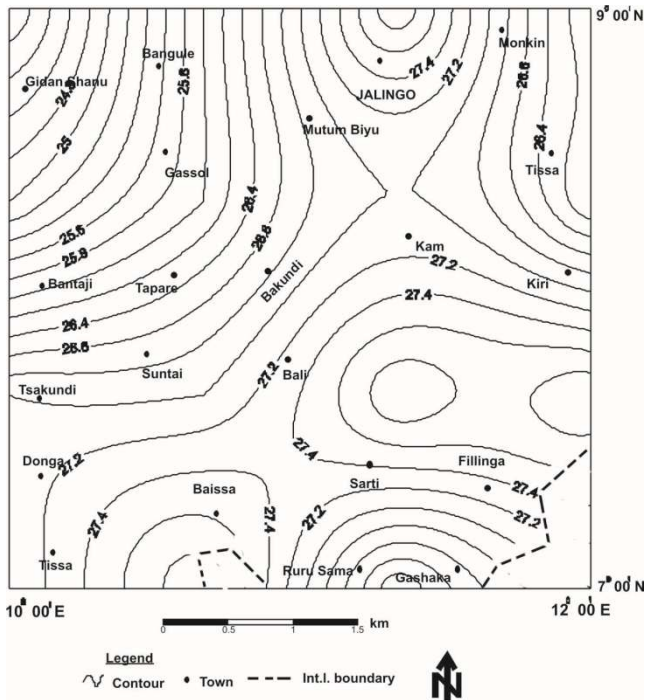


Figure 7: Curie isotherm map of the study area (contour interval of 0.1nT)

The 2D curie depth profile A-A (figure 8) beneath the study area was determined from a spectral analysis technique, which showed that the Curie point surface is undulating and deepens from 24 km in the west to 28 km in the east (Figure 9)

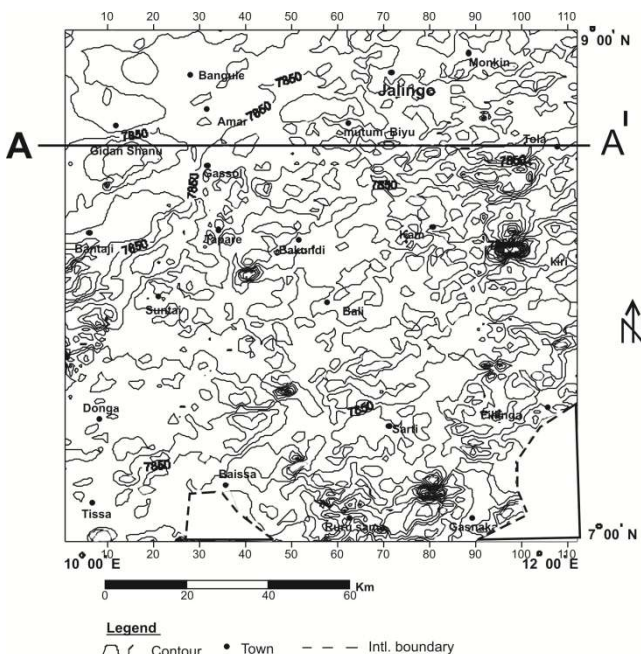


Figure 8: Total intensity contour map showing the profile A-A from which 2-D was plotted. (Contour interval of 50nT).

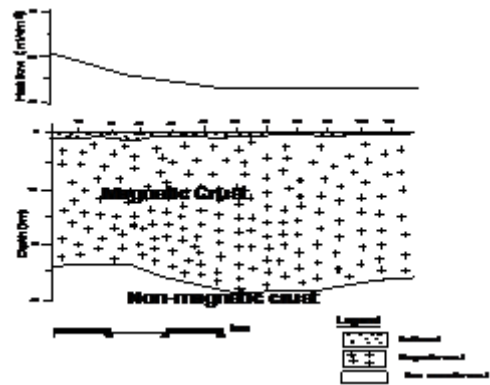


Figure 9: 2D Curie point depth and heat flow anomaly section for profile A-A

5. Discussion of Result

The mineralization of rocks depends on their chemical composition and various tectonic episodes that have affected the rocks. Considering that fact, the total magnetic intensity (Fig.2) over Jalingo and environs after the digitization, showed magnetic signature ranging from 7500nT to 8145nT.

The magnetic susceptibility contrasts across fracture zones are due to oxidation of magnetite to hematite, and /or infilling of fracture planes by dyke like bodies whose magnetic susceptibilities are different from those of their host rocks [1], Such geological features appear as thin elliptical closures or nosing on the residual magnetic map (Fig.3). Bearing this in mind, prominent elliptical closures and nosing were identified on the analytical signal map from Hilbert transformation; this transformation sharpens the edges of anomalies and enhances the anomalous features. The features / lineaments identified are represented by lines drawn parallel to the closure and /or elongation of the anomalies. The lineaments map deduced from analytical signal indicated that 53% trend NE-SW; 28% NW-SE; 12% E-W and 7% N-S direction as illustrated by azimuth (Rose diagram) Figure 5. These correspond to Pan-African and Pre-Pan-African deformational episodes in the study area

Looking at figure 4, the analytical signals concentrated more in the south and south eastern part of study area. This may be explained as; the basement complex outcropping here is not mineralogically homogeneous. The contoured map (Fig.2) shows the presence of remarkable magnetic features, which agree quite well when compared with geologic map of (Fig.1)

Magnetic source depth determination through spectral analysis over Jalingo and environs suggests two main source depths. The deepest source lies between 437m to 2617m and the shallower source depths obtained range from 123m to 436m. These could be as a result of intrusive bodies from Cameroon Volcanic line in the study area. Table1 shows the computed magnetic source depths in the area. The areas of thick overburden/ weathered basement are potential site for ground water exploration. The result is also in line with previous work obtained from gravity and magnetic analysis by several authors among which are: [17] estimated the sediment thickness in Upper

Benue, which range from 500m to 4600 m. "Ref. [22]" estimated sediment thickness, which ranges from 900 m to 2200 m from gravity data interpretation, and 900 m to 4900m from magnetic data. "Ref.[12]" also estimated the sediment thickness, which ranges between 1500m to 2219 m for deeper source, and range between 330m to 414m for shallow source.

Graphs of the logarithms of the spectral energies, from which Curie isotherm depth was computed, showed that the depth to the Centroid (Z_c) ranges from 12.520 km to 16.100 km. On the other hand, the depth to the top boundary (Z_t) of magnetic sources ranges from 1.030 km to 4.980 km (below sea level) Table 1.

The equivalent curie depth range from 24 km to 28 km (b.s.l), these values compares well with what was obtained in Upper Benue Trough by [11]. The obtained Curie point depth reflects the average local curie depth point values beneath each block. It is observed that the curie depth in the North-Western part of the study is moderately shallower (24-26 km) compared to the other part of the area, these reflect the thinning of the crust under Benue rift. It is also observed that, volcanic areas on the geologic map Fig.1 have moderately shallow Curie point depth of 26km compared to the other basement areas; this could be as result of upwelling of magma on Cameroon Volcanic line (CVL). The deeper Curie point in the centre of the study area could be as a result of isostatic compensation in the region. The obtained Curie point was used to construct curie isotherm map of the study area (Fig 7). These reflect the various depths to curie points which describe the thermal nature of the crust. Previous studies by [24] showed that the Curie point depth is linked to the geological context of an area Spectral analysis of the data in conjunction with heat flow values revealed an almost inverse linear relationship between heat flow and Curie depths (Fig 6), these were used to construct Curie isotherm from the existing data. In most part of the study area, heat flows were found to be less than 60 mWm^{-2} This implies that the heat flows in the study area are not uniform, which possibly indicate that the magma conduits were randomly distributed.

The average heat flow obtained in the study area is 55.010 mWm^{-2} , this may be considered as typical of continental crust.

All the current literatures state that the curie point depth and of course heat flow is greatly dependent upon geological conditions. Heat flow is the primary observable parameter in geothermal exploration. Generally, the units that comprise of high heat flow values correspond to Volcanic and metamorphic regions since the two rock units have high heat conductivities [15]. It is In view of this, the volcanic areas on geologic map of the study area Figure.1, as well as metamorphic region beneath the Benue rift show moderate heat flow of the magnitude of 60 mWm^{-2} above.

6. Conclusion

The analysis of the aeromagnetic data over Jalingo and its environs indicated the existence of two magnetic source depths; the deepest source lies between 437m to 2617m

and shallower source depth obtained ranges from 123m to 436m and could be attribute of intrusive bodies.

The structural lineaments/fractures observed from the analytical signals of Hilbert transformed data of the study area are dominantly in NE-SW, NW-SE, E-W and N-S direction and are potential site for secondary mineralization in the study area. These were presented by azimuth (Rose diagram) in terms of magnitude and direction which showed that, 53% trend NE-SW; 28% NW-SE; 12% E-W and 7% N-S. Most high magnitude lineaments could be attributed to deep seated fractures, while the low magnitude could be attributed to shallow weathered zones in the area. The azimuth magnitudes and the trend of the fractures are in line with the Pan-African and Pre-Pan-African deformational episodes in the area. However areas of thick overburden are potentials site for ground water exploration.

The Curie point depth for the study area was estimated using surface magnetic data through spectral analysis. The inferred Curie point depth which described the thickness of the crust obtained in the study area ranges from 24 km to 28 km. The result reveals that, the Curie point depth varies inversely with heat flow; this shows that heat flow in the study area decreases with increase in Curie depth. 2D Curie point surface under profile A-A shows that is undulating and deepens from 24 km to 28 km (Figure 9) In addition to that, Curie depth in the study area is moderately shallower under the Benue rift in the North-Western part with an average heat flow of 55.010 mWm^{-2} . These resulted from the rifting of Benue Trough and upwelling of the asthenosphere which is responsible for the generation of thermal dome in volcanic centres. The results compared favourably with what was obtained by [11]. It confirms that Curie depths are indirect indicator of the thermal structure of an area.

The interpretation of aeromagnetic data to estimate the depth to Curie point isotherm and heat flow over Jalingo and environs, contributed to the better understanding of geothermal regime and tectonic activities in this area, which shows a possibility for geothermal resources potentials to explore for new and more energy locations in Nigeria.

7. Acknowledgment

The authors are Grateful to the geological survey Agency of Nigeria for releasing the aeromagnetic maps. Authors are also grateful to Prof. Markku P. of Olu University Finland, Department of Geophysics for providing FOUT POT software which was used for processing the aeromagnetic data.

References

- [1] Basseyy, N. E. Nur, A. and Obiefuna, G. I., 2000. Analysis of Aerial Photographic data over Guyuk area, North-eastern Nigeria, Journal of Mining and Geology, Vol. 36, (2), pp. 45-152.
- [2] Bhattacharryya, B.K. and L.K. Leu., (1975). Spectral analysis of gravity and Magnetic anomalies due two

- dimensional structures, *Geophysics*, Vol. 40, PP 993-1031
- [3] Ekwueme, B.N., 1994. Structural features of southern Obudu plateau, Bamenda massif, SE Nigeria, Preliminary Interpretation. *Jour. Mining. Geol.* Vol. 30, (1), PP. 45 - 59.
- [4] Nigeria Geological Agency, 1975, Air Bone Magnetometer Survey Contour Map of Total Magnetic Field Intensity of Nigeria
- [5] Nigerian Geological Agency, 2006, Geological map of Nigeria
- [6] Grant, N.K., 1978. Structural distinction between a metasedimentary cover and underlying basement in 600 m.y old Pan-African domain of northwest Nigeria, *West African Geol. Sic. Am. Bull.* 89, PP 50 - 58
- [7] Hahn, A. E., Kind, G., and Mishra, D.C., 1976. Depth estimation of magnetic sources by means of Fourier amplitude spectra. *Geoph. Prospect* Vol. 24, PP 287 – 309
- [8] Hisarli, Z. M., (1996). Determination of Curie Point Depths in Western Anatolia and Related with the Geothermal Areas, Ph.D. Thesis, Istanbul University, Turkey (unpubl.), (in Turkish with English abstract).
- [9] Kasidi, S and Nur, A., (2012). Analysis of aeromagnetic data over Mutum- Biyu and Environs, North-Eastern Nigeria, *Research Journal in Engineering and applied sciences*, Vol. 2 (1), PP.142 - 148.
- [10] Markku, P., 2009. Fourier transform based processing of 2D potential field data Version 1.0a (software). Division of Geophysics, Department of Geosciences FIN-90014 University of Oulu Finland
- [11] Nur, A, Ofoegbu C.O. and Onuoha K.M., 1999, Estimation of the depth to the Curie point Isotherm in the upper Benue trough, Nigeria, *Jour. Min. Geol.* Vol. 35 (1), PP 53 - 60.
- [12] Nur, A., 2000. Analysis of aeromagnetic data over Yola arm of the Benue Trough, Nigeria, *Mining and Geol.* Vol. 36 (1), PP 77 - 84
- [13] Nur A, Kamurena, E and Kasidi S., 2011, Analysis of Aeromagnetic data over Garkida and Environs, North-Eastern Nigeria, *Global Journal of Pure and applied Sciences*, Vol. 17 (2), PP 209 - 214
- [14] Nuri D, M. Timur U, Z. Mumtaz H, and Naci O., (2005), Curie Point Depth variations to infer thermal structure of the crust at the African-Eurasian convergence zone, SW Turkey. *Journ. Earth planets Space* Vol 57, PP 373-383
- [15] Nwankwo, L.I, Olasehinde, P.I and Akoshile, C.O., (2011). Heat flow anomalies from the spectral analysis of Airborne Magnetic data of Nupe Basin, Nigeria. *Asian Journal of Earth Sciences*, Vol.1. No.1, PP 1-6
- [16] Offodile, M.E., 1977. A review of the geology of the cretaceous Benue Trough in *Geology of Nigeria* (Ed. Kogbe, C.A), Elizebeth press Lagos PP 319-330..
- [17] Ofoegbu, C.O., 1988. An aeromagnetic study of part of the Upper Benue Trough, Nigeria, *Jour. Afr. Earth Sci.* Vol. 7, PP 77 - 90.
- [18] Ofoegbu, C.O., and Mohan, N.I., 1990. Interpretation of aeromagnetic anomalies over parts of south eastern Nigeria using three dimensional Hilbert transformations, *Pageoph*, Vol. 134, PP 13-29
- [19] Ofoegbu, C.O. and Onuoha, K. M., 1991. Analysis of magnetic data over the Abakaliki Anticlinorium of the lower Benue Trough, Nigeria, *Marine and Petr. Geol.* Vol. 8, PP 174 - 183.
- [20] Ofoegbu, C.O, Odigi, M.I. Okereke, C.S. and Ahmed, N.M., 1992, Magnetic anomalies and the structure of the Nigeria's Oban massif: *Journal. of African Earth Sciences*, Vol. 15 (2), PP 217 - 280.
- [21] Okubo, Y.J. R. Graf, R. O. Hansen, K. Ogawa, and, H. Tsu., (1985). Curie point depth of the Island of Kyushu and surrounding areas, *Japan Geophysic.* Vol 53 PP 481-491.
- [22] Osazuwa, I.B., Ajakaiye, D. E and Verheijin, P.J.T., 1981. Analysis of the structure of part of the Benue Valley on the basis of new geophysical data, *Earth Evol Sci.*, Vol. 2, PP 126-135
- [23] Spector, A. and Grant, F.S., 1970, Statistical models for interpreting aeromagnetic data, *Geophysics*, Vol. 35, PP 293 - 302
- [24] Stampolidis, A. Kane, I., Tsokas G.N. and Tsourlo P., (2005). Curie point depths of Albania inferred from ground total field magnetic data, *Surveys in Geophysics.* Vol. 26, PP 461-480
- [25] Stefan, M., and Vijay, D., 1996, Depth estimation from the scaling power spectrum of potential fields?. *Geophysics, J. Int.*, Vol.124, PP 113-120
- [26] Tanaka, A., Y. Okubo, and O. Matsubayashi., (1999). Curie point depth based on spectrum analysis of the magnetic anomaly data in East and Southeast Asia, *Tectonophysics*, Vol. 306, PP 461-470
- [27] Tselentis, G.A (1991), An attempt to define Curie depth in Greece from Aeromagnetic and heat flow data, *PAGEOPH*, Vol. 136, No. 1, PP 87-101